Feasibility Demonstration of a Mode-Division Multiplexed MIMO-enabled Radio-over-Fiber Distributed Antenna System

George S.D. Gordon, *Student Member, IEEE,* Michael J. Crisp, *Member, IEEE,*
Richard V. Penty, *Senior Member, IEEE,* Timothy D. Wilkinson, *Senior Member, IEEE,*
and Ian H. White, *Fellow, IEEE*

***Abstract*—In this paper the feasibility of *mode-division multiplexing (MDM)* for implementing *multiple-input multiple-output (MIMO) radio-over-fiber (RoF) distributed antenna systems (DAS)* is experimentally demonstrated, where the MIMO algorithm is able to reconstruct the data signals by overcoming distortion and cross-talk in both the free-space RF and optical fiber channels. This is achieved through RF characterization of an MDM RoF link, which is experimentally demonstrated to be capable of supporting at least 4×4 MIMO with 6GHz channels over long lengths of MMF (2km compared to $\sim$300m typically found in MMF-based RoF DASs) and under tight fiber bending conditions (bend radius as low as 7.6mm), which are commonly encountered in in-building fiber installations.**

First, experimental RF measurements are performed over a 2km section of OM2 fiber, mode-multiplexed using a *spatial light modulator (SLM)* based MUX/DEMUX system, and it is shown to offer an RF condition number of $<$14dB for up to 4×4 MIMO with 6GHz channels, sufficient to enable good performance for most modern wireless protocols. Next, the effect of fiber curvature on RF performance is experimentally analysed using a 10m section of OM3 fiber. It is seen that with a bend radius as low as 7.2mm, a condition number of ~ 10dB can be achieved for up to a 6×6 MIMO system with 6GHz channels.

Although an SLM-based MUX/DEMUX is used here, condition number is not dependent on the exact mode-launching system used provided that orthogonal combinations of modes are excited, which is true of most MDM systems. It is therefore concluded that the RF characterization presented here demonstrates by proof-of-principle the feasibility of *graded-index (GI)* MMF to support at least 4×4 MIMO with broadband channels via MDM over lengths up to 2km and with fiber bend radii as low as 7.2mm.

***Index Terms*—MIMO, distributed antenna systems (DAS), radio-over-fiber (RoF), mode multiplexing**

I. Introduction

The number of wireless devices is at an all-time high with an estimated 6.8 billion mobile subscriptions and 1.5 billion WLAN capable devices worldwide [1]. This has driven a huge increase in usage of wireless data, the demand for which is predicted to increase 13 fold from 2012-2017 [2]. As a result, it is forecast that in the next few years the capacity load on wireless networks will outstrip supply by as much as 90% [3]. This is of particular importance in indoor environments where an estimated 80-90% of wireless data traffic originates [4].

To avert this shortfall wireless protocols have been continually improving, for example by using high-order modulation, *orthogonal frequency-division multiplexing (OFDM)* and advanced coding schemes, such that their performance is now approaching the theoretical Shannon capacity limit. More recently, wireless systems have benefited from the introduction of *multiple-input multiple-output (MIMO)* schemes, in which multiple transmit and receive antennas are used with *spatial multiplexing (SM)* algorithms, such as V-BLAST, to create additional parallel communication channels [5].

However, even MIMO protocols are now approaching the theoretical limits of spectral efficiency [6]. The next frontier in increasing the capacity of mobile networks is to redesign wireless network infrastructure to incorporate a higher density of radio-access points. A number of methods are commonly employed to do this, the most popular being femtocells, relays and *distributed antenna systems (DAS)*. In a DAS the RF antenna feeds from multiple collocated wireless base stations are transported to remotely located antennas. DASs have been used for some time to provide indoor coverage improvement [7] and are a popular in-building technology with over 89,000 installations worldwide [8].

Many DASs transport RF feeds to remote antennas using *radio-over-fiber (RoF)* technology, in which radio signals are modulated onto optical carriers and sent down optical fibers. Because RoF is intrinsically broadband, it can support multiple services or multiple cells of a single service over the same DAS infrastructure [9]. Today's indoor wireless services use a wide range of frequencies – from *terrestrial trunked radio (TETRA)* used by government agencies and emergency services operating just below 400MHz, to IEEE 802.11n and 802.11ac operating in the 5GHz band. A broadband DAS, operating up to at least 6GHz is then desirable so that all these services, as well as others that have not yet been developed, can be provided simultaneously using the same infrastructure. The ability to support multiple cells on a single DAS also makes possible intelligent cell reconfiguration, a unique feature of DASs that makes them a powerful method of adding capacity to an indoor wireless network.

II. MIMO-enabled RoF DAS

To provide maximum capacity benefit, future DASs must support high-capacity MIMO protocols. It has been shown that in systems with small numbers of MIMO spatial streams, typically ≤ 4, distributing these MIMO streams amongst separately located *remote antenna units (RAUs)* provides similar

The authors are with Electrical Engineering Division, University of Cambridge, CB3 0FA, Cambridge, U.K. (e-mail: gsdg2@cam.ac.uk).

performance to the case of sending all MIMO streams to every RAU [10]. The former method has the significant advantage that existing non-MIMO DAS infrastructure can be re-used with little modification to support MIMO protocols. However, for MIMO protocols with larger numbers of spatial streams, such as 802.11ac with up to 8 streams, it is necessary to send multiple spatial streams to each RAU in order to maximize SNR of each spatial stream and hence achieve maximum MIMO performance.

The availability of additional transmitting antennas beyond the number of spatial streams also enables additional performance improvements, especially if the radio *channel state information (CSI)* is fed back to the transmitter [11]. Further, the ability to form precise beams in systems with large arrays of transmit antennas, termed *large scale antenna systems (LSAS)*, has been shown to simultaneously improve capacity and reduce energy usage [12]. Future DAS will thus require the ability to send multiple MIMO streams occupying the same frequency space to a single RAU.

This could be achieved simply by installing additional fibers for the extra streams. However, this is an expensive approach as the installation cost of new fiber in a building can be substantial and is often not practically feasible. A more cost-effective solution is to re-use existing DAS infrastructure, or existing cabling installed for other services such as Ethernet.

Several methods have been proposed to send MIMO streams over existing DAS infrastructure. Sub-carrier multiplexing and other RF frequency translation techniques have been experimentally proven to be effective [13]. However, these techniques necessarily use up additional portions of the available RF spectrum, which prevents truly multiservice operation. Wavelength division multiplexing (WDM) has been proposed as a potential solution to support larger numbers of streams [14], [15]. This approach enables the transmission of multiple broadband MIMO streams but has the disadvantage of additional complexity and cost, although this is an inherent problem with many multiplexing schemes. Polarization-division multiplexing (PDM) has also been experimentally demonstrated to support 2×2 MIMO RoF for mm-wave signals over a single-mode fiber [16].

A more recent innovation is the idea of using *mode-division multiplexing (MDM)*, in which different spatial modes of a multimode fiber (MMF) are used to transport independent data streams – in this case the RF spatial streams transmitted by a wireless MIMO system. An example 8×8 MIMO RoF DAS using MDM is shown in Figure 1. MDM has recently gained much attention in data transmission applications as a means to overcome the capacity limits of optical fibers [17].

Simulation work has shown the feasibility of using multiple offset-launched optical channels, each exciting orthogonal combinations of mode-groups, to implement broadband MIMO RoF links [18]. More recently, experimental work has demonstrated MDM supporting broadband 2×2 MIMO RoF up to 6GHz over a single 2km section of OM2 MMF [19]. A major advantage of this last system is that it is able to multiplex modes of OM1,OM2 and OM3 GI MMF, of which there is approximately 17 million km installed in buildings worldwide [20].

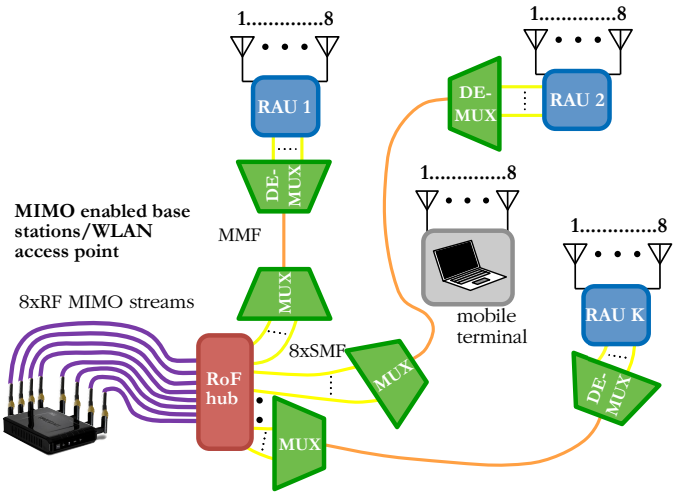

Fig. 1. Diagram showing a the layout of an 8×8 MIMO-enabled RoF DAS using mode-division multiplexed MMF to feed RAUs.

Because wireless MIMO SM algorithms, such as V-BLAST, use periodic channel estimation any additional linear cross-talk or attenuation introduced by coupling between modes in an MDM RoF link is accounted for in the same way as similar effects in the wireless propagation channel. This only works if the fiber channel is linear, but for typical RoF links the low optical powers used and the limited bandwidths of individual RF services within the spectrum mean that nonlinear effects in the fibre can be considered negligible, as discussed further in Section III. Therefore, minor system misalignments or fiber defects causing mode-coupling are compensated for by the wireless MIMO and no additional *digital signal processing (DSP)* is required. Further, coherent optical detection is not required as the phase of the modulated RF signal is preserved by commonly-used optical envelope detectors, such as photodiodes.

In this paper the RF transfer characteristics of spatially multiplexed MMFs over long lengths and under a range of bending conditions are measured. Using an SLM-based mode-launcher and receiver system, groups of modes with similar propagation constants, termed *mode-groups* are launched and received, and the cross-coupling between them is analyzed.

First, the importance of condition number as a performance metric for MIMO channels is discussed. It is shown that a condition number, an indication of the separability of spatial channels, of $<$20dB for an MDM RoF channel is sufficient to enable it to support wireless MIMO protocols in a typical indoor propagation environment.

Next, it is shown experimentally that for a 2km length of OM2 fiber, the modal selectivity of an SLM-based spatial MUX/DEMUX and the mode-coupling within the fiber are sufficient to support up to 4×4 MIMO with a condition number of $<$14dB over an RF bandwidth of 6GHz. To the best knowledge of the authors this is the longest distance achieved for 4×4 MIMO RoF operation over multimode fiber.

Following this, the RF transfer characteristics of a 10m length of OM3 fiber are examined with a range of fiber bend radii down to 4.6mm. Unlike in long-haul underground

installations, fiber installed inside buildings is often inadvertently forced around tight corners or is pinched and bent. Such bends reduce the performance of mode-multiplexing as they attenuate high-order modes. It is observed that as bend radius is decreased, power in the higher-order mode groups decreases by up to 8dB due to loss into the cladding and increased coupling to other mode-groups. However, the condition number is measured at ∼10dB for up to a 6×6 MIMO system with RF channels of 6GHz bandwidth and with a bend radius of ≥7.1mm. This shows the feasibility of providing broadband 6×6 MIMO under tight fiber bend radii. To the authors' knowledge, this is the first experimental investigation of the effects of fiber bend radius on the RF characteristics of modal propagation.

In this case, the MUX/DEMUX is implemented using an SLM-based system, but other lower cost and lower loss schemes, for example employing *photonic lanterns*, are suitable candidates for future commercial mode-multiplexing systems [21]. However, irrespective of the exact MUX/DEMUX scheme used, all MDM systems rely on the excitation of particular subsets of fiber modes. Condition number as presented here is in fact independent of the particular choice of launch/receive modes used for multiplexing and instead depends on the fundamental properties of the transmission channel and the fiber, particularly mode-coupling. Given this, the results presented here together show for generalized MDM systems that over long-lengths of MMF (up to 2km) and under conditions of significant bending (bend radius up to 7.1mm) it is possible to provide at least 4×4 broadband MIMO RoF over a single MMF.

III. Theory

Wireless MIMO channels are modelled as linear communication channels in which a complex vector of M input symbols, $\mathbf{x}$, is mapped to a complex vector of N output symbols, $\mathbf{y}$, by an $N \times M$ matrix of complex coefficients, $\mathbf{H}$, termed the *channel matrix*. $\mathbf{H}$ represents the transfer function of the propagation channel and its elements are random variables that model the effect of multipath fading. In the case of *fast-fading* with a flat frequency response over the bandwidth of the RF service (i.e *flat fading*) and assuming channel state information (CSI) is not available at the transmitter, the theoretical Shannon capacity of the channel is given by [22]:

$$C = \log_2 \det \left(\mathbf{I} + \frac{\rho}{M} \mathbf{H} \mathbf{H}^H \right) \tag{1}$$

where ρ is the average signal-to-noise ratio (SNR) of the link. The inclusion of a MIMO-enabled RoF link in the channel downlink can be modelled as an additional $M \times M$ channel matrix multiplied by the wireless channel matrix:

$$\mathbf{H} = \mathbf{H}_{\text{prop}} \mathbf{H}_{\text{RoF}} \tag{2}$$

where $\mathbf{H}_{\text{prop}}$ is the free-space radio propagation channel matrix and $\mathbf{H}_{\text{RoF}}$ is the transfer matrix of the RoF link. For example, in the case of a mode-multiplexed fiber link, $\mathbf{H}_{\text{RoF}}$ represents the coupling matrix between each of M launched modes (or mode-groups) and M received modes (or mode-groups).

This model assumes that the mode-multiplexed fibre channel is linear but in reality, there are several mechanisms that introduce nonlinearity. At high optical powers non-linear modal cross talk is observed due to dynamic changes in refractive index [23]. Experimental work has shown that optical powers of the order of 16dBm are typically required to induce high-power nonlinear mode-coupling in few-mode fibers [24]. Given that RoF systems typically use optical powers of ∼0dBm, this mechanism is not likely to cause observable linearity here. Further, the OM2 and OM3 fibers used here have core diameters of 50μm compared with $\sim 10\mu$m found in few-mode fibers, which substantially reduces the cross-sectional optical power density and hence nonlinearity of the fiber.

Nonlinear behaviour can also occur when the coherence bandwidth of a mode-multiplexed fiber is less than the bandwidth of the modulated signal [25]. Over 2km of OM2, as used in this work, the coherence bandwidth across all modes is ∼1.25GHz [26]. However, because typical broadband RoF signals actually comprise multiple independent narrowband (<40MHz) RF signals, the frequency response of the fibre channel need only be flat within each service. This requirement is easily met as the bandwidths of RF services are typically an order of magnitude less than the coherence bandwidth of a mode-multiplexed fiber. Further, many modern wireless protocols apply OFDM within their allocated bandwidth, which essentially equalizes this non-flat spectrum. Consequently, in this paper the mode-multiplexed fiber channel can be considered to be linear.

In order not to reduce the capacity of the link, $\mathbf{H}_{\text{RoF}}$ must be unitary [22]. If that is the case, the DSP algorithms built into the wireless MIMO protocols are able to fully reverse any cross-coupling between modes occurring in the fiber. DSP algorithms used in digital data transmission MDM systems must also include time-delay filters with many taps to compensate for the *differential mode delay (DMD)* between mode-groups, which can cause *intersymbol interference (ISI)*. However in MIMO wireless protocols such as 802.11n, symbols are typically 3.2μs in duration and a guard interval of 0.4 or 0.8μs is inserted to allow for the differential delay of spatial streams without causing ISI. Therefore, a tap-length of 1 sufficient and the DSP algorithm simply inverts the channel matrix.

Ideal multimode fibers have unitary channel matrices but in reality there will be non-unitary mixing between modes due to imperfections in mode launching and detection, lossy fiber bends and imperfections over longer distances. The degree to which a matrix is unitary can be measured by the *condition number*, K, of the channel matrix H, expressed as:

$$K = \frac{\max\limits_{p}(\sigma_p)}{\min\limits_{p}(\sigma_p)} = \|\mathbf{H}^{-1}\| \|\mathbf{H}\| \tag{3}$$

where σ_p represents the p^{th} singular value of the channel matrix H, $\max\limits_{p}(\sigma_p)$ represents the maximum σ_p across all p, $\min\limits_{p}(\sigma_p)$ represents the minimum σ_p across all p, and $\|\mathbf{H}\|$ is the L^2-norm of $\mathbf{H}$. Because the L^2-norm obeys the sub-

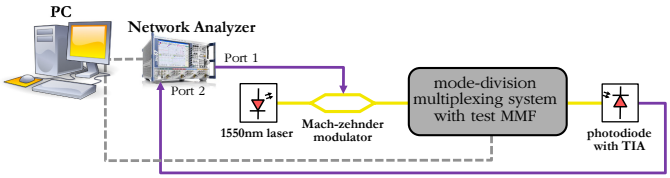

Fig. 2. Experimental set-up for RF characterization of mode-division multiplexed RoF link.

multiplicative property, we observe:

$$\|\mathbf{H}\| \leq \|\mathbf{H}_{\text{prop}}\|\|\mathbf{H}_{\text{RoF}}\| \tag{4}$$

$$\|\mathbf{H}^{-1}\| \leq \|\mathbf{H}_{\text{RoF}}^{-1}\|\|\mathbf{H}_{\text{prop}}^{-1}\| \tag{5}$$

Combining Equations 3, 4 and 5, it is seen that an upper bound can be placed on the overall condition number:

$$K \leq K_{\text{prop}} K_{\text{RoF}} \tag{6}$$

where K_{prop} and K_{RoF} are the condition numbers of $\mathbf{H}_{\text{prop}}$ and $\mathbf{H}_{\text{RoF}}$ respectively. It should be noted that in MDM literature, the condition number of a multimode fiber channel (i.e. K_{RoF}) is termed *mode-dependent loss (MDL)*. Further, it is also possible to derive a lower bound on the condition number:

$$K \geq \max\left(K_{\text{prop}}, K_{\text{RoF}}\right) \tag{7}$$

Condition number is often expressed in dB as $K_{\text{dB}} = 20\log_{10}(K)$. For a realistic indoor wireless propagation environment, the median K_{dB} is typically around 20dB, giving a linear value of $K = 10$ [10]. In order that the RoF channel has minimum impact on overall condition number, it is desirable that the lower bound, as per Equation 7, be limited by K_{prop}, requiring $K_{\text{RoF}} \leq 10$. Therefore, when designing a RoF link, a reasonable target for K_{RoF} is that it should be less than 10 (20dB) but ideally as small as possible. However, a tighter limit on K used in other literature is that $K_{\text{dB}} \leq 10$, as this is the point beyond which SNR starts to be the dominant factor affecting capacity, rather than conditioning of the channel [27]. In this work then, the ideal RoF condition number sought is $K_{\text{RoF}} \leq$10dB, but less than 20dB is still considered acceptable as it does not affect the lower bound of K in a typical indoor environment.

IV. Experimental set-up

The experimental set-up used to measure the RF channel characteristics of the mode-division multiplexing system is shown in Figure 2. A Mach-Zehnder Modulator (MZM) is used to amplitude modulate the RF test signal from the vector network analyzer (VNA) onto an optical carrier at 1550nm. Though this is an inherently nonlinear modulation scheme, because the VNA receiver has a narrowband filter ($\sim$ 10MHz) at the input to port 2, the harmonic terms are filtered out and so only the linear response is measured. There are negligible intermodulation distortion (IMD) terms because the VNA sweeps through frequencies one at a time.

A schematic of the all-optical mode-division multiplexed link is shown in Figure 3. This particular implementation supports simultaneous transmission of up to two modes - LP_{01}, and an arbitrary higher-order mode. Linear combinations of higher-order modes, e.g. entire mode-groups, are also possible on the second channel by displaying a superposition of phase-masks. The phase mask are displayed on 2 SLMs - a 512×512 binary-phase SLM at the MUX and a 1920×1080 nematic phase SLM with 256 phase levels at the DEMUX.

It is relatively straightforward to add additional channels by incorporating a fiber array at the MUX, similar to that used at the DEMUX. When a blaze grating is superimposed on the SLM (equivalent to adjusting the *tilt* aberration term), beams incident on the SLM from slightly offset fibers can be manipulated individually before being focussed onto the MMF [28]. In fact, the architecture used at the DEMUX can simply be used in reverse to implement this.

Provided the fibers in the array are not too far offset from the central optical axis, each channel should offer similar performance. The main source of cross-talk between channels is optical misalignment or aberrations in the system, imperfections in the phase masks used, which assume ideal fiber propagation modes, and coupling due to long lengths or bends in fibers. These effects are also present to the same degree when examining modal cross-talk within a single channel. This is because the channels are separated at the transmitter and receiver using mode-selective phase masks displayed on the SLM, which are used in a very similar way for separating multiple channels and analysing a single channel. Therefore, in this work, only a single channel (Channel 2) is characterized and the RF and optical transfer coefficient is measured for every possible combination of transmit and receive phase masks. This measurement gives an indication of performance that includes all the mechanisms of cross-talk mentioned above. The only deviation expected from this in practice is increased optical aberrations in channels that use fibers in the array further from the central optical axis. However, even this is largely corrected for using automatic aberration correction algorithms as discussed below.

It should also be noted that while the DEMUX can analyse two polarizations independently, the MUX can only launch modes in a single polarization. However, a single polarization is still sufficient for an initial analysis of spatial coupling effects as presented here, particularly given that polarization is expected to change unpredictably over a long length of fibre and around tight bends, both of which are key elements of this work.

Before being used, the MDM system is aligned using a single-mode fiber. A blaze grating is superimposed on the phase-mask and is adjusted to direct light from the SLM onto fibers and vice-versa, allowing adjustment for slight differences between fibers. Next, a steepest-descent search is used to find appropriate Zernike polynomials that, when superimposed on the phase-masks, correct for common aberrations - defocus, spherical, astigmatism and coma. A single-mode fiber (SMF) is used in place of the MMF for this stage and the search is terminated when the power coupled into it is maximized [28].

Once the system is aligned, the VNA is then calibrated.

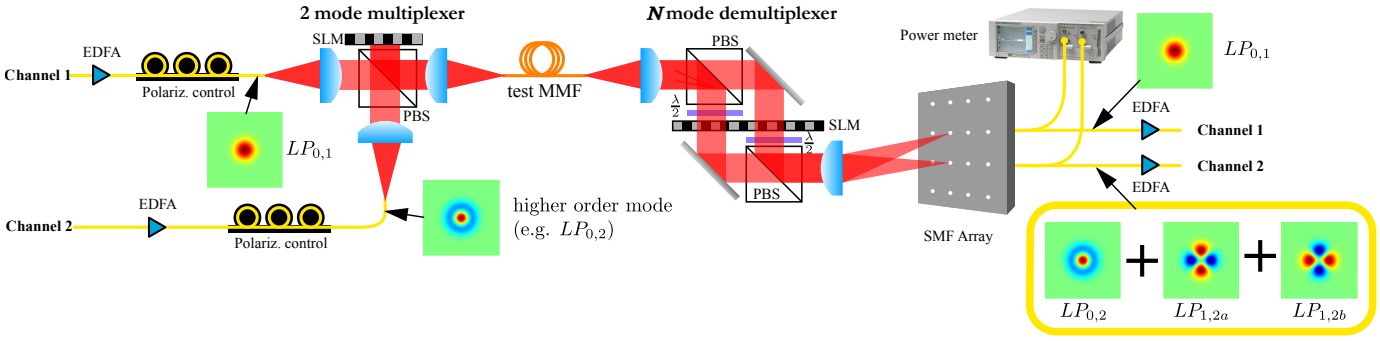

Fig. 3. Experimental set-up of SLM-based multiplexer/demultiplexer.

For the through measurement, a back-to-back measurement of the full system (excluding the SLMs is taken). This allows for compensation of frequency effects arising in the MZM and in the photodiode receiver. For each sweep taken by the VNA, the optical power meters, shown in Figure 3, record the received power before the EDFAs. This enables optical power-coupling matrices to be examined for each test condition. This differs from the RF measurements in that the EDFAs used at the receiver have *automatic gain control (ACG)*, so that differences in power when different modes are transmitted are compensated. These power differences are typically of the order of 8-9dB between the highest and lowest order modes. This difference is due to different conversion efficiencies of phase masks for different modes - some are more lossy than others - but the main driver is increased leakage into other modes when using high-order modes. In a practical RoF system, such ACG would instead be implemented in the RF amplifiers at the RAU and so EDFAs might not be required.

In a silica GI MMF, coupling between individual modes within the same mode-group (i.e. with the same propagation constant) is very high compared with coupling between modes in different mode-groups [29]. As a result, if any particular mode is launched, after only a short distance of fiber it couples much power into other modes in the same mode-group, as illustrated in Figure 3. Because of this, many real MDM systems multiplex between mode-groups [26]. The transmit phase masks are able to launch all the modes in a single group with approximately equal power, and at the receiver the phase masks are set to coherently add all the modes in the same mode-group together so as to maximize power. This is possible due to the coherent nature of the phase-only SLMs. This effect can be simulated by aggregating the full measured mode transfer matrix over entire-mode groups with coherent summation at the DEMUX SLM. If there are N mode groups this then results in an $N \times N$ *mode-group transfer matrix*. In this work, the RF measurements are aggregated into frequency dependent mode-group transfer matrices and these are used to assess the potential of the system to provide MIMO RoF, presented in the next section.

The first fiber tested is a 2km spool of OM2 fiber, the purpose of which is to demonstrate the feasibility of long distance operation. Next, it is desired to gain experimental insight into the impact of fiber bending on modal propagation in mode multiplexing systems. In order to achieve this several makeshift mandrels were constructed using pieces of dowel of different radius, as listed in Table I. Also listed is the curvature, κ, defined as $1/r$ where r is the bend radius of the fiber. A 600mm section of a 10 metre OM3 multimode fiber patchcord is wrapped around each of these pieces of dowel in turn.

There are in fact minimum recommended bend radii specified in industry standards for particular kinds of fiber in order to avoid performance degradation. For example the Telecommunications Industry Association states that the minimum bend radius of a fiber should be no less than 10 times the cable diameter, about 32mm for standard OM1-OM4 cables. The actual breaking point of fibers is much smaller – a loop of radius 5mm has a breakage probability of less than 10^{-5}. However, in real installations it is not always practically feasible to meet these recommendations given space constraints and it is often difficult to measure fiber bend radii. Furthermore, the positions of fibers are liable to change during building maintenance and upgrading. Given this, it is expected that the values used here would be commonly found in many realistic installations.

TABLE I
RADII OF DOWEL USED FOR TESTING FIBER UNDER DIFFERENT BEND CONDITIONS.

Dowel radius (mm)	**Fiber bend radius (mm)**	**Curvature κ (mm^{-1})**
(straight fiber)	∞	0.0000
19.2	20.8	0.048
12.9	14.5	0.069
9.9	11.5	0.087
7.5	9.1	0.111
5.6	7.2	0.139
3.0	4.6	0.217

V. RESULTS

A. 2km OM2 test

The measured optical power coupling matrix for the 2km of OM2 fiber is shown in Figure 4. The values are normalized to the total received power across all modes to compensate for the effect of the different coupling efficiencies of each launched mode. It can be seen that while good power confinement is achieved for low-order mode-groups (1-4), there

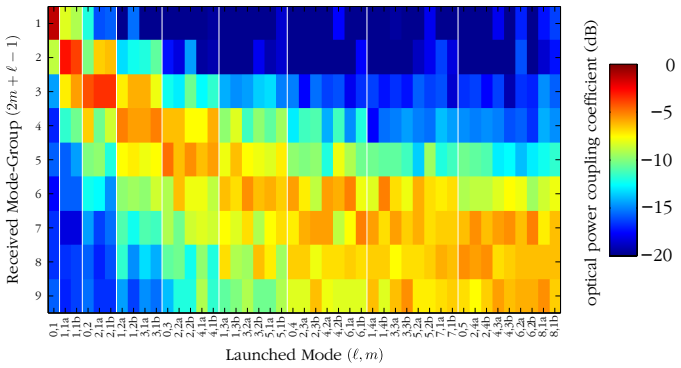

Fig. 4. Measured mode power coupling matrix for 2km OM2 fiber. The x-axis represents the launched mode, while the y-axis is the received power summed within each mode-group.

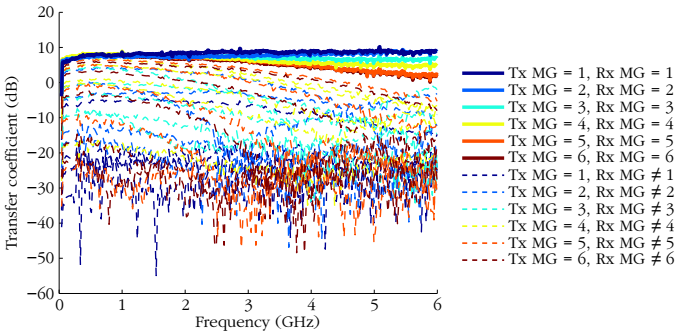

Fig. 5. RF coupling coefficients between mode-groups over 2km of OM2 fiber.

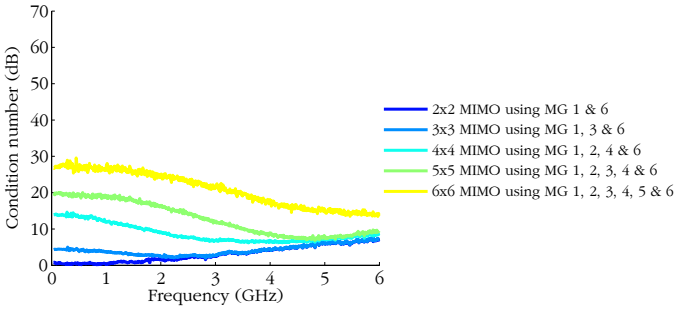

Fig. 6. RF condition number over 2km of OM2 fiber.

is significantly higher cross-coupling between the high order mode-groups.

The RF power coupling coefficients for the first 6 mode-groups measured over the 2km OM2 fiber are shown in Figure 5. It is observed that for the first 3 mode-groups, there is typically $<$ 6dB isolation ratio – that is, the ratio of power received within the same mode-group to power received in other mode-groups. This decreases significantly for the high-order mode-groups. Because of the mode-selective launch, modal dispersion is minimized and each channel is seen to have a very high bandwidth (a bandwidth-distance product of $\sim$12GHz.km). However, some high-frequency roll-off is observed for the high-order mode-groups due to cross-coupling effects in the fibre introducing modal dispersion.

Because the MUX SLM is not optimized for operation at 1550nm, it has a high optical insertion loss of $\sim$20dB. The DEMUX SLM, by contrast, has an optical insertion loss of $<$5dB and it should be possible to replicate this at the MUX in future designs. The EDFAs are each set to have an optical gain of $\sim$15dB. Since the modulation index of the MZM is set to be close to 1, this results in a net system optical gain of $\sim$5dB, corresponding to an RF signal gain of $\sim$10dB, which is observed in Figure 5.

However, it is also seen that the RF condition number, plotted in Figure 6, is $<$14dB for up to the 4×4 MIMO case. This indicates that although there is significant cross-talk, it can be largely reversed by use of DSP SM algorithms, such as those used in wireless MIMO protocols. The condition number is seen to deteriorate for the 5×5 and 6×6 MIMO cases. It is noted that over this distance of fiber the delay between the highest and lowest order mode-groups is of the order of 700-900ps, corresponding to a phase-shift of up to 4λ between the RF spatial streams. As a result, the condition number in Figure 6 varies with frequency due to different relative phase shifts of different spatial streams. This is not observed for shorter fiber lengths as in Figure 11. This delay spread is well within the tolerance of 802.11n, which allows at least 400ns, and so does not create significant ISI.

B. Fiber bending test

Next, the optical power coupling matrix for an unbent 10m patch cord of OM3 fiber is measured, as shown in Figure 7. It can be seen that the power is much better confined in each mode-group than for the 2km OM2 case, with isolation ratios $>$6dB up to mode-group 6 and 7. However, when the patch cord is bent, significant changes occur. The total received power across all mode-groups for different launched mode-groups as fiber curvature is increased is shown in Figure 8. It is seen that with no bending the total power across all mode-groups is lower for higher mode-groups, which is largely due to less efficient transmit and receive phase masks. However, when the fiber is bent to a radius of 4.6mm, the highest order mode-groups experience significant additional power loss (up to 8dB), while mode-groups 1-4 remain largely unaffected. It is noted, that for a slightly larger bend radius (7.2mm) only mode-groups 7-9 are affected significantly by the curvature.

The isolation ratio of each mode-group, that is, the ratio of power received in the transmitted mode-group to power in other mode-groups is shown in Figure 9. Three distinct classes of behaviour are observed. The first is mode-groups whose behaviour does not change, demonstrating their robustness under tight bending, namely mode-groups 1-4. The second class is observed in mode-groups 5-7 where the isolation ratio initially improves with increased bend radius. This is due to increased power coupled back into these mode-groups due to bending and also because power leaked out of them into higher-order mode-groups is heavily attenuated by dissipation into the cladding. The third class of behaviour observed in mode-groups 8 and 9 is when the dominant behaviour resulting from bending is mode-group power being dissipated into the

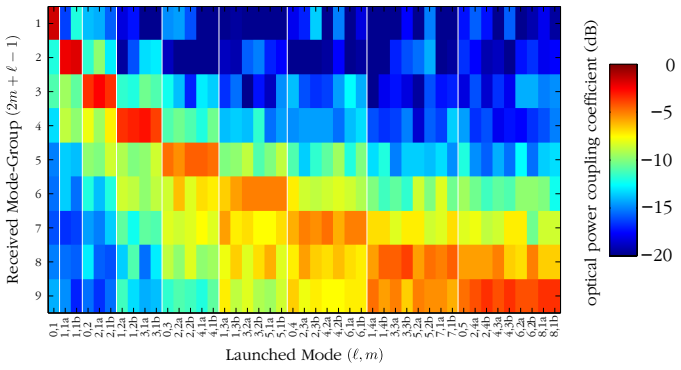

Fig. 7. 10m unbent OM3 fiber mode power coupling matrix.

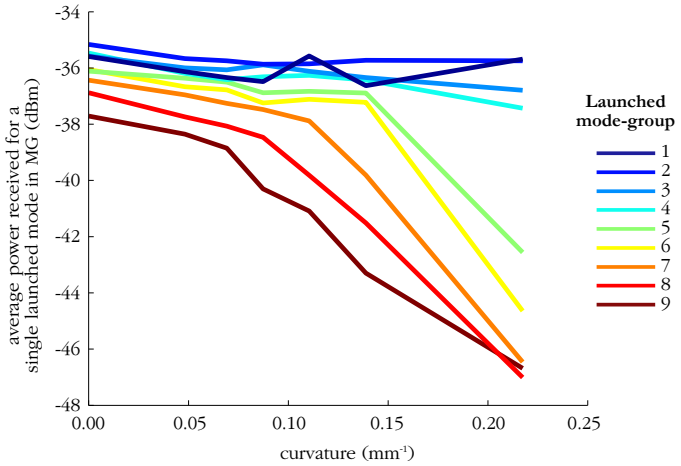

Fig. 8. Total received power aggregated across all mode-groups for different launched mode groups as fiber curvature is increased. This indicates that power is lost into the cladding from the higher order modes as fiber curvature is increased.

cladding. This graph also shows limits that represent the expected isolation ratios if power were distributed equally amongst all mode-groups. When the isolation ratio of a mode-group drops below this threshold, sufficient power is lost from the mode-group that subsequent measurements have a substantial random component and do not necessarily represent trends.

The RF coupling coefficients of the fiber bent to a radius of 4.6mm are shown in Figure 10. It can be seen that performance starts to deteriorate significantly when mode-group 6 is used, and in that case the power coupled to other mode-groups is significantly larger than that confined to the launched mode-group.

The condition number of this fiber when supporting 6×6 MIMO is plotted for different curvatures in Figure 11. In this case, it is seen that the condition number is $\sim$10dB for a bend radius $<$7.2mm, indicating very favourable MIMO channel properties. However, there is a substantial increase to $\sim$30dB beyond this.

VI. Conclusion

This paper demonstrates for the first time, by way of proof-of-principal experimental RF characterization of an optical fiber link, that mode-division multiplexing is a feasible method

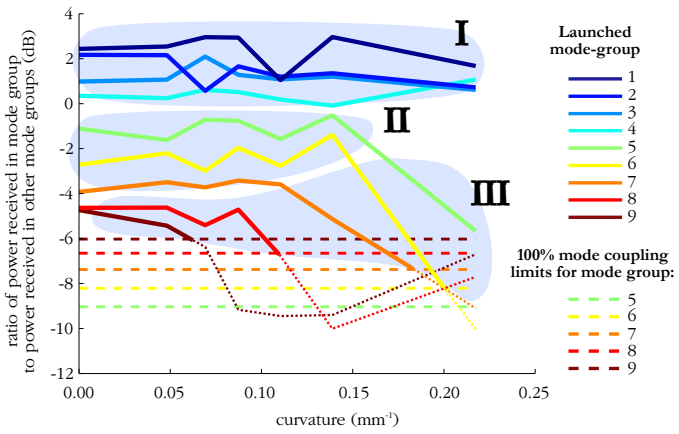

Fig. 9. Ratio of the power received in the same mode-group as is launched to the power received in other mode-groups. As the fiber curvature is increased, three different classes of behaviour are observed: I - mode-groups unaffected by curvature, II - mode-groups with increased isolation ratio due to increased power coupling into them from other mode-groups and/or additional attenuation of power leaked out of them, III - decreasing isolation ratio due to loss of power into cladding.

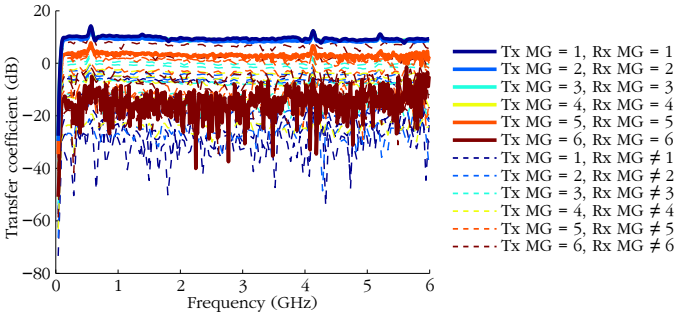

Fig. 10. RF coupling coefficients between mode-groups over 10m of OM3 fiber at a 4.6mm bend radius.

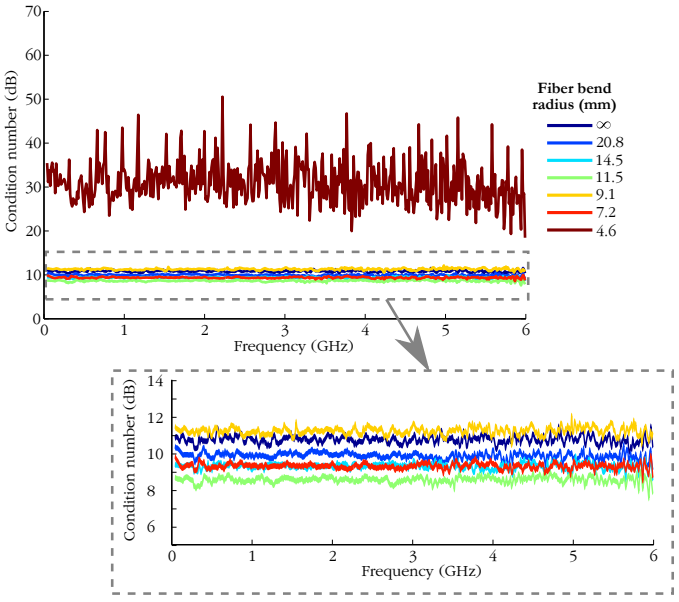

Fig. 11. Condition number of 10m OM3 fiber as curvature is increased for a 6×6 MIMO system using mode-groups 1-6.

of providing multiple broadband RF MIMO channels over a

single MMF for application in a RoF DAS. It is shown that a condition number of < 14dB can be achieved for a 4×4 MIMO system with 6GHz wide channels over 2km of OM2 fiber. It is then shown that with a bend radius as small as 7.2mm a condition number of $\sim$10dB can be achieved for a 6×6 MIMO system with 6GHz wide channels over 10m of OM3. These values show that both links are sufficient to enable good performance for most modern wireless MIMO protocols. Together, these results demonstrate the feasibility of mode-multiplexing systems using standard OM2 and OM3 fiber to provide broadband MIMO RoF channels over existing in-building fiber infrastructure that may include long lengths and tight bends, without the need to install additional fiber.

ACKNOWLEDGEMENT

The authors would like to thank Dr. Joel Carpenter, the U.K. Engineering and Physical Sciences Research Council (EPSRC) and the Quaternian project, funded by the EU 7th Framework Programme, for their support.

REFERENCES

[1] "Measuring the Information Society," International Telecommunication Union, Tech. Rep., 2013.

[2] "Cisco Visual Networking Index : Global Mobile Data Traffic Forecast Update , 2012 2017," Cisco Systems, Tech. Rep., 2012.

[3] "Visible light communication (vlc) - a potential solution to the global wireless spectrum shortage," GBI Research, Tech. Rep., 2011.

[4] T. Norman, "Research forecast report - Wireless network traffic 2010-2015: forecasts and analysis," Analysys Mason, Tech. Rep., 2010.

[5] D. Gesbert, M. Shafi, P. Smith, and A. Naguib, "From theory to practice: an overview of MIMO space-time coded wireless systems," *IEEE Journal on Selected Areas in Communications*, vol. 21, no. 3, pp. 281–302, Apr. 2003.

[6] "Spectral Efficiency," Qualcomm, Tech. Rep., 2009.

[7] M. J. Crisp, S. Li, R. Penty, A. Watts, and I. H. White, "Uplink and Downlink Coverage Improvements of 802.11g Signals Using a Distributed Antenna Network," *Journal of Lightwave Technology*, vol. 25, no. 11, pp. 3388–3395, Nov. 2007.

[8] "Femtocells and Distributed Antenna Systems Complementary or Competitive?" ABI Research, Tech. Rep., 2009.

[9] D. Wake, A. Nkansah, and N. J. Gomes, "Radio Over Fiber Link Design for Next Generation Wireless Systems," *Journal of Lightwave Technology*, vol. 28, no. 16, pp. 2456–2464, Aug. 2010.

[10] G. Gordon, M. Crisp, R. Penty, and I. White, "Experimental Evaluation of Layout Designs for 3x3 MIMO-Enabled Radio-over-Fiber Distributed Antenna Systems," *IEEE Transactions on Vehicular Technology*, no. c, pp. 1–1, 2013.

[11] G. S. D. Gordon, M. J. Crisp, R. V. Penty, and I. H. White, "Experimental Investigation of Antenna Selection and Transmit Beamforming for Capacity Enhancement in," in *International Topical Meeting on Microwave Photonics 2013*, 2013.

[12] H. Yang and T. L. Marzetta, "Performance of Conjugate and Zero-Forcing Beamforming in Large-Scale Antenna Systems," *IEEE Journal on Selected Areas in Communications*, vol. 31, no. 2, pp. 172–179, Feb. 2013.

[13] A. Chowdhury, H.-c. Chien, J. Wei, and G.-k. Chang, "Multi-service Multi-carrier Broadband MIMO Distributed Antenna Systems for In-building Optical Wireless Access," in *Optical Fiber Communication (OFC), collocated National Fiber Optic Engineers Conference, 2010 Conference on (OFC/NFOEC)*, 2010, pp. 26–28.

[14] A. van Zelst, "System for transporting multiple radio frequency signals of a multiple input, multiple output wireless communication system to/from a central processing base station," *US Patent App. 10/195,504*, 2004.

[15] K. Miyamoto, T. Tashiro, T. Higashino, K. Tsukamoto, S. Komaki, K. Hara, T. Taniguchi, J.-i. Kani, N. Yoshimoto, and K. Iwatsuki, "Experimental demonstration of MIMO RF signal transmission in RoF-DAS over WDM-PON," *2011 International Topical Meeting on Microwave Photonics jointly held with the 2011 Asia-Pacific Microwave Photonics Conference*, pp. 25–28, Oct. 2011.

[16] A. Kanno, T. Kuri, and I. Hosako, "Optical and millimeter-wave radio seamless MIMO transmission based on a radio over fiber technology," *Optics Express*, vol. 20, no. 28, pp. 29 395–29 403, 2012.

[17] D. J. Richardson, "Applied physics. Filling the light pipe." *Science (New York, N.Y.)*, vol. 330, no. 6002, pp. 327–8, Oct. 2010.

[18] M. Awad, I. Dayoub, W. Hamouda, and J.-M. Rouvaen, "Adaptation of the Mode Group Diversity Multiplexing Technique for Radio Signal Transmission Over Multimode Fiber," *Journal of Optical Communications and Networking*, vol. 3, no. 1, p. 1, Dec. 2010.

[19] G. Gordon, J. Carpenter, M. Crisp, T. Wilkinson, R. Penty, and I. White, "Demonstration of Radio-over-Fibre Transmission of Broadband MIMO over Multimode Fibre using Mode Division Multiplexing," in *European Conference and Exhibition on Optical Communication*, no. 1, 2012.

[20] A. Flatman, "In-Premises Optical Fibre Installed Base Analysis to 2007," 2007. [Online]. Available: http://www.ieee802.org/3/10GMMFSG/public/mar04/flatman_1_0304.pdf

[21] N. K. Fontaine, R. Ryf, S. G. Leon-Saval, and J. Bland-Hawthorn, "Evaluation of Photonic Lanterns for Lossless Mode-Multiplexing," in *European Conference and Exhibition on Optical Communication*. Optical Society of America, 2012, p. Th.2.D.6.

[22] D. Tse and P. Viswanath, *Fundamentals of Wireless Communication*. Cambridge: Cambridge University Press, 2005.

[23] G. Rademacher, S. Warm, and K. Petermann, "Analytical Description of Cross-Modal Nonlinear Interaction in Mode Multiplexed Multimode Fibers," *IEEE Photonics Technology Letters*, vol. 24, no. 21, pp. 1929–1932, Nov. 2012.

[24] R.-J. Essiambre, M. a. Mestre, R. Ryf, A. H. Gnauck, R. W. Tkach, A. R. Chraplyvy, Y. Sun, X. Jiang, and R. Lingle, "Experimental Investigation of Inter-Modal Four-Wave Mixing in Few-Mode Fibers," *IEEE Photonics Technology Letters*, vol. 25, no. 6, pp. 539–542, Mar. 2013.

[25] J. M. Kahn, "Frequency Diversity in Mode-Division Multiplexing Systems," *Journal of Lightwave Technology*, vol. 29, no. 24, pp. 3719–3726, Dec. 2011.

[26] J. Carpenter, B. Thomsen, and T. Wilkinson, "Degenerate Mode-Group Division Multiplexing," *Journal of Lightwave Technology*, no. c, pp. 1–1, 2012.

[27] E. Ohlmer, J. Hofrichter, S. Bittner, G. Fettweis, Q. Wang, H. Zhang, K. Wolf, and D. Plettemeier, "Urban Outdoor MIMO Experiments with Realistic Handset and Base Station Antennas," in *2010 IEEE 71st Vehicular Technology Conference*. Ieee, 2010, pp. 1–5.

[28] J. Carpenter, B. C. Thomsen, and T. D. Wilkinson, "Mode Division Multiplexing of Modes With the Same Azimuthal Index," *IEEE Photonics Technology Letters*, vol. 24, no. 21, pp. 1969–1972, Nov. 2012.

[29] R. Olshansky, "Mode Coupling Effects in Graded-index Optical Fibers." *Applied optics*, vol. 14, no. 4, pp. 935–45, Apr. 1975.